Single-photon threshold photoionization of NO

Ralph T. Wiedmann, Michael G. White, Kwanghsi Wang, and V. McKoy

Citation: The Journal of Chemical Physics **98**, 7673 (1993); doi: 10.1063/1.464575
View online: http://dx.doi.org/10.1063/1.464575
View Table of Contents: http://scitation.aip.org/content/aip/journal/jcp/98/10?ver=pdfcov
Published by the AIP Publishing

Single-photon threshold photoionization of NO

Ralph T. Wiedmann and Michael G. White
Brookhaven National Laboratory, Chemistry Department, Upton, New York 11973

Kwanghsi Wang and V. McKoy
Arthur Amos Noyes Laboratory of Chemical Physics,[a] California Institute of Technology, Pasadena, California 91125

(Received 18 December 1992; accepted 3 February 1993)

Single-photon threshold photoionization spectra for jet-cooled NO have been measured for the $v^+=0$ and 1 vibrational levels of the $X\,^1\Sigma^+$ ground state of NO^+. The NO^+ rotational state distribution for the $v^+=0$ level is shown to be perturbed by nearby autoionizing levels, whereas the $v^+=1$ level exhibits a cation rotational distribution which is in near quantitative agreement with calculated spectra near threshold. Only small changes in total angular momentum are observed ($|\Delta J|=|J^+-J''|\leqslant 5/2$) even though a wide range of photoelectron angular momenta ($l=0$–3) are predicted to contribute to the near-threshold photoelectron continua. The present results are also discussed in light of recently published two-photon threshold photoionization spectra of NO which exhibit nearly identical NO^+ rotational state distributions.

I. INTRODUCTION

The dynamics of photon-induced fragmentation processes are most often inferred from measurements of the asymptotic states and spatial distributions of the products. For photoionization leading to a molecular ion and a photoelectron, high-resolution electron spectroscopy can in principle provide a complete quantum-state characterization of the products since all the recoil momentum is carried away by the light photoelectron "fragment." Such analyses require measurement of the rotational state distribution of the resulting cation which is usually beyond the resolution capabilities of conventional photoelectron spectrometers with electrostatic or time-of-flight analyzers. By working with high rotational levels ($J\sim J^+\geqslant 20$) where the spacings of adjacent lines are relatively large ($\sim 80\ cm^{-1}$), Reilly and co-workers were able to obtain rotationally resolved photoelectron spectra of NO^+ produced from resonance enhanced multiphoton ionization (REMPI) via the Rydberg states of NO.[1] This work as well as parallel *ab initio* theoretical studies[2,3] demonstrated the utility of rotationally resolved measurements for characterizing the underlying dynamics of photoionizing transitions. More recently, Reid *et al.*[4] have shown that all the dynamical parameters, including scattering phase shifts, required to specify the photoionization step in the (1+1) REMPI via the $A\,^2\Sigma^+$ ($3s\sigma$) of NO can be extracted from a combination of rotationally resolved photoelectron spectra and angular distributions.

With the recent development of zero-kinetic-energy (ZEKE) photoelectron techniques, it is now possible to obtain cation rovibronic state distributions with sub-wavenumber resolution.[5] Although ZEKE techniques are limited to measurements of threshold photoionization cross sections, a wider range of molecular cations can be studied in an effort to explore the coupling of electronic and nuclear motions inherent in the photoionization process. Using a variant of the ZEKE technique based on delayed pulsed-field-ionization (PFI) of high-n Rydberg states,[6,7] we have measured the ion rotational state distributions for single-photon ionization of a number of systems including O_2 (Refs. 7 and 8), N_2O (Ref. 9), H_2O (Refs. 10 and 11), H_2S (Refs. 12 and 13), OH (OD) (Ref. 14), and HCl (Ref. 15). For the most part, comparisons with simulations based on the one-electron, line strength expressions derived by Buckingham *et al.*[16] as well as with *ab initio* calculated spectra have established that the observed PFI rotational branch intensities directly reflect the partial wave distributions of the photoelectron continua. Conservation of angular momentum limits the allowable changes in total angular momentum to $\Delta J=J^+-J''=l+3/2$, $l+1/2,\ldots,-l-3/2$, where J'' and J^+ are the total angular momenta of the ground and ionic states, respectively, and l is an angular momentum component of the photoelectron.[17] In the case of O_2, an f wave shape resonance in the σ_u photoelectron continuum near threshold enhances the $l=3$ contribution leading to the observation of rotational branches with $|\Delta J|$ as large as 9/2 (Refs. 8 and 18). In contrast, the threshold spectra for H_2O are dominated by rotational transitions with small changes in total angular momentum ($|\Delta J|\leqslant 3/2$) due to the dominance of low-l partial waves.[11,19]

In this work, we present threshold photoelectron spectra for the $v^+=0$ and 1 vibrational levels of the $X\,^1\Sigma^+$ ground state of NO^+. These data are interpreted on the basis of *ab initio* calculations of the near-threshold rotational state branching ratios. In these calculations, multiplet-specific static-exchange potentials associated with final-state wave functions are included to properly describe the photoelectron continuum orbitals near threshold. In studies of rotationally resolved photoelectron spectra at low photoelectron kinetic energies, it is essential to use such photoelectron orbitals so as to faithfully represent the actual angular momentum coupling. Unlike the exam-

[a]Contribution No. 8771.

 0021-9606/93/107673-07$06.00

ples cited above, threshold photoionization of NO represents a case of "spectator" ionization in which angular momentum exchanges between the escaping photoelectron and ion core are small ($|\Delta J| \leqslant 5/2$), despite large $l=2$ and 3 photoelectron transition amplitudes. The perturbations in the spectrum of the $v^+=0$ level due to rotational autoionization are discussed in relation to previous examples observed in N_2O (Ref. 9), OH (Ref. 14), and HCl (Ref. 15). The present single-photon ionization data for NO are compared to very recent two-photon, nonresonant ZEKE threshold photoelectron spectra of Strobel *et al.*[20] Surprisingly, the one- and two-photon spectra are quite similar, despite the obvious difference in angular momentum balance between the two measurements. The implications of these results will also be discussed.

II. EXPERIMENTAL DETAILS

The photoelectron spectrometer and free-jet vacuum ultraviolet (VUV) radiation source have been described in detail elsewhere.[21] Essentially, we use a small, separately pumped frequency-tripling chamber attached to a molecular beam photoelectron/photoion time-of-flight (TOF) spectrometer. Tunable VUV radiation in the range 133.9–129.6 nm required to reach the $v^+=0$ and 1 vibrational levels of the $X\ ^1\Sigma^+$ ground state of NO^+ was produced by resonant, four-wave difference-frequency mixing ($2\omega_{uv}-\omega_{vis}$) in Kr gas using the $5p[2\frac{1}{2}]_{J=2} \leftarrow \leftarrow 4p$ two-photon resonance at 92 308.2 cm^{-1} (Refs. 22 and 23). The 216.7 nm radiation (ω_{uv}) was produced by sum-frequency mixing the first and second harmonics of a Nd:YAG-pumped, dye laser (Quanta-Ray PDL-3, Continuum YG-680, 20 Hz) using DCM dye. A second Nd:YAG-pumped, dye laser (Quanta-Ray PDL-1, Quanta-Ray DCR-2A, 20 Hz) was used to produce the visible difference-frequency light (ω_{vis}) with Rhodamine 590 dye for $v^+=0$ and DCM dye for $v^+=1$. Relative timing between the two Nd:YAG lasers was maintained to better than ± 2 ns by controlling the lamp and Q-switch triggers via a high precision external timing generator (EG&G 9650). The collinear visible and UV laser beams were focused by a 100 mm focal length achromatic lens (Optics for Research) into a pulsed, free-jet expansion of Kr inside the tripling chamber. The diverging fundamentals (visible and UV) and VUV radiation were captured by a Pyrex capillary light guide (30 cm long; 1 mm i.d.) and directed into the TOF spectrometer, where they pass between two parallel plates which define the extraction field for the TOF spectrometer. The sum (910−930 nm) and difference (133.9−129.6 nm) frequency VUV radiation were separated by using a small flow of Xe gas (~0.5 Torr) directed into the center of the capillary light guide. The dilute Xe gas distributed over the length of the capillary makes an effective absorption filter for the sum-frequency radiation due to its relatively high absorption cross section (~60 Mb) near and above the $^2P_{1/2}(5p)^{-1}$ excited state ionization threshold (13.436 eV, 92.28 nm).[24] The VUV intensity at the spectrometer is estimated to be $\sim 10^9$ photons/pulse, with an energy bandwidth of $\sim 0.5\ cm^{-1}$.

The molecular beam is prepared for the experiment by expanding 800–1000 Torr of a 2%–5% mixture of NO in Ar into the source chamber ($\sim 3\times 10^{-4}$ Torr) through a pulsed valve (Laser Technics) fitted with a 0.5 mm diam nozzle. A 1 mm skimmer located 0.5 cm downstream of the valve collimates the beam so that it passes cleanly through the TOF apparatus (background pressure with sample is $\sim 1\times 10^{-5}$ Torr).

High-resolution threshold spectra were obtained by the delayed PFI method first demonstrated by Reiser *et al.*[6] PFI takes advantage of the well known Stark shift of an ionization threshold in an external electric field (given by $\sim 6\sqrt{F}\ cm^{-1}$, where F is the field strength in V/cm). Bound Rydberg levels very near the ionization threshold which are stable in a field-free environment become open ionization channels when a Stark shift larger than their binding energy is applied. For fields used in this work (0.3–0.6 V/cm) only Rydberg levels with $n \geqslant 150$ can be field ionized. Rydberg states with such high principal quantum numbers are very long-lived due to rapid l mixing induced by a small dc electric field (~0.05–0.15 V/cm).[25] The small dc voltage applied to the repeller plate also sweeps out any slow or near-ZEKE photoelectrons produced directly by the laser pulse. After a delay of 700 ns, a fast, negative pulse ranging in amplitude from 0.3–0.6 V was applied to the repeller plate. Electrons produced by pulsed field ionization are readily distinguished from direct photoelectrons by the arrival-time dependence on the pulse delay. After passing through a 30 cm field-free region, the electrons are detected by a dual microchannel plate multiplier and TOF spectra are recorded by a CAMAC controlled 200 MHz transient digitizer (LeCroy 8828D).

III. THEORY AND NUMERICAL DETAILS

A. Theory

The general theory of molecular photoionization processes used in the present studies has been described previously.[26,27] Here we present just a very brief outline of some essential features of our procedure as it is used to obtain rotationally resolved photoelectron distributions. Under collision-free conditions, ionization originating from each of the $(2J_0+1)$ magnetic sublevels of the initial state forms an independent channel. Therefore, the total cross section σ for ionization of a J level of the initial state leading to a J^+ level of the ion can be written as[26]

$$\sigma \propto \sum_{\substack{lm \\ M_J M_{J+}}} \rho_{M_J M_J} |C_{lm}(M_J M_{J+})|^2, \tag{1}$$

where $\rho_{M_J M_J}$ is the population of a specific M_J level of the initial state. The coefficients $C_{lm}(M_J M_{J+})$ of Eq. (1) are related to the probability for photoionization of the M_J level of the initial state leading to the M_{J+} level of the ionic state. An expression for $C_{lm}(M_J M_{J+})$ which explicitly considers the spin coupling associated with multiplet-specific final-state wave functions and an intermediate coupling scheme between Hund's cases (a) and (b) for the initial and ionic states has been given by Wang and

McKoy.[26] For the branching ratios of interest here, the constant implied in Eq. (1) is unimportant and will be suppressed.

A central quantity in these studies is the matrix element for photoejection of an electron from a bound molecular orbital ϕ_i into a photoelectron continuum orbital $\Psi_{f,\mathbf{k}}^{(-)}(\mathbf{r})$. Here $\mathbf{k}$ is the momentum of the photoelectron and $(-)$ denotes incoming-wave boundary conditions. The partial wave components $\psi_{klm}^{(-)}$ of $\Psi_{f,\mathbf{k}}^{(-)}(\mathbf{r})$ are defined by an expansion in spherical harmonics about $\hat{\mathbf{k}}$,

$$\Psi_{f,\mathbf{k}}^{(-)}(\mathbf{r})=\left(\frac{2}{\pi}\right)^{1/2}\sum_{lm} i^l\psi_{klm}^{(-)}(\mathbf{r})\,Y_{lm}^*(\hat{\mathbf{k}}). \tag{2}$$

Single-center expansions of $\psi_{klm}^{(-)}(\mathbf{r})$ and $\phi_i(\mathbf{r}')$, e.g.,

$$\psi_{klm}^{(-)}=\sum_{l'\lambda} g_{lm,l'\lambda}(k,r)\mathscr{D}_{m\lambda}^{l'}Y_{l'\lambda}(\hat{\mathbf{r}}'), \tag{3}$$

define partial wave photoelectron matrix elements $r_{fi}^{l\lambda\mu}$ in the molecular frame for ionization out of orbital $\phi_i(\mathbf{r}')$, i.e.,

$$r_{fi}^{l\lambda\mu}=\sum_{l',l_0}\langle g_{lm,l'\lambda}(k,r)\,Y_{l'\lambda}(\hat{\mathbf{r}}')\,|\,rY_{1\mu}(\hat{\mathbf{r}}')\,|\,\phi_{il_0}(r)\,Y_{l_0,\lambda_0}(\hat{\mathbf{r}}')\rangle, \tag{4}$$

where μ is the photon polarization index in the molecular frame, m and λ are the projection of l in the laboratory and molecular frames, respectively, and $\mathscr{D}_{m\lambda}^{l}$ is a rotational matrix in Edmonds' notation.[28] Equation (4) reveals an important underlying dynamical aspect of molecular photoelectron wave functions. Whereas only $l=l'$ terms are allowed in Eq. (4) for the central fields of atomic systems, where the angular momentum of the photoelectron must be conserved, $l\neq l'$ terms arise in Eq. (4) due to the nonspherical potential fields of molecular ions. This angular momentum coupling between partial waves l and l' is brought about by the torques associated with the molecular ion potential and makes a molecular photoelectron orbital an admixture of angular momentum components. These angular-momentum changing collisions between the photoelectron and molecular ion play a crucial role in rotationally resolved molecular photoelectron spectra. The use of molecular photoelectron orbitals which correctly incorporate such angular momentum coupling is essential at the low photoelectron energies of interest here.

B. Numerical details

The ground state wave function of NO used here is obtained at the self-consistent-field (SCF) level at the equilibrium internuclear distance of $R_e=2.1746\ a_0$.[29] We used a basis of (9*s*5*p*/5*s*3*p*) contracted Cartesian Gaussian functions[30] augmented with one *s*, one *p*, and one *d* (polarization) functions centered on the nuclei (with exponents 0.1, 0.08, and 1.0 at the nitrogen atom and 0.12, 0.09, and 1.0 at the oxygen atom, respectively) and two *s*, two *p*, and one *d* functions at the center of mass with exponents 0.0453 and 0.011 41 for the *s* functions, 0.044 and 0.0167 for the *p* functions, and 0.1626 for the *d* functions. The total SCF energy in this basis was $-129.275\,901$ a.u. The single-center expansion of the 2π orbital around the center of mass gives 2.81% *p*, 84.42% *d*, 1.04% *f*, 9.93% *g* ($l_0=4$), 0.15% *h* ($l_0=5$), and 1.29% *i* ($l_0=6$) character.

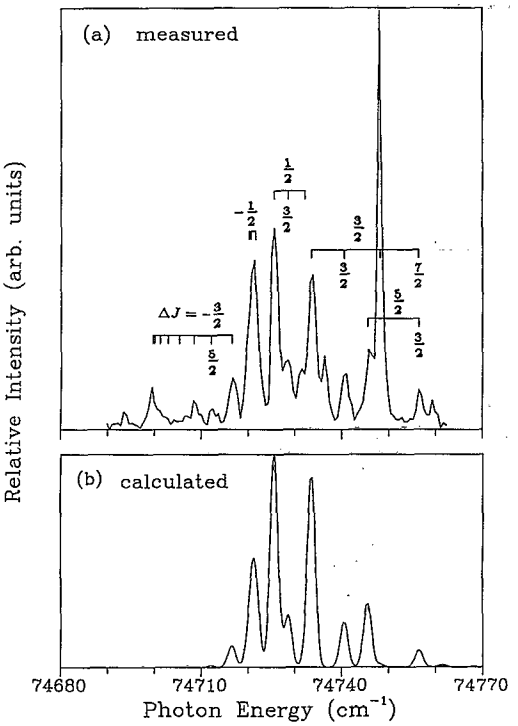

FIG. 1. (a) Measured and (b) calculated rotationally resolved threshold PFI photoelectron spectra for the single-photon ionization transition NO^+ $[X\,^1\Sigma^+(v^+=0,J^+)]+e^-\leftarrow NO$ $[X\,^2\Pi_{1/2}(v''=0,J'')]$. The rotational branch labels refer to $\Delta J=J^+-J''$. The calculated photoelectron spectrum assumes a ground state rotational temperature of 5 K.

For the final state we assume a frozen-core Hartree–Fock model in which the core orbitals are taken to be those of the ion and the photoelectron orbital is obtained as a solution of a one-electron Schrödinger equation containing the Hartree–Fock potential of the molecular ion, $V_{\text{ion}}(\mathbf{r},R)$, i.e.,

$$\left(-\tfrac{1}{2}\nabla^2+V_{\text{ion}}(\mathbf{r})-\frac{k^2}{2}\right)\psi_{klm}^{(-)}=0, \tag{5}$$

where $k^2/2$ is the kinetic energy of the photoelectron. To obtain the partial wave photoelectron orbitals $\psi_{klm}^{(-)}$, we use an iterative procedure, based on the Schwinger variational principle, to solve the Lippmann–Schwinger equation associated with Eq. (5).[31] Three iterations provided highly converged solutions for the molecular photoelectron orbitals. Further details of calculations can be found in Ref. 32.

IV. RESULTS AND DISCUSSION

The measured PFI threshold photoelectron spectra for single-photon ionization of rotationally cold NO in the $X\,^2\Pi_{1/2}(v''=0)$ ground state to the $v^+=0$ and 1 levels of the $X\,^1\Sigma^+$ ground ionic state are shown in Figs. 1(a) and 2(a), respectively. These spectra were obtained with a 2% mixture of NO in Ar at an 800 Torr stagnation pressure in the pulsed valve. These expansion conditions resulted in a

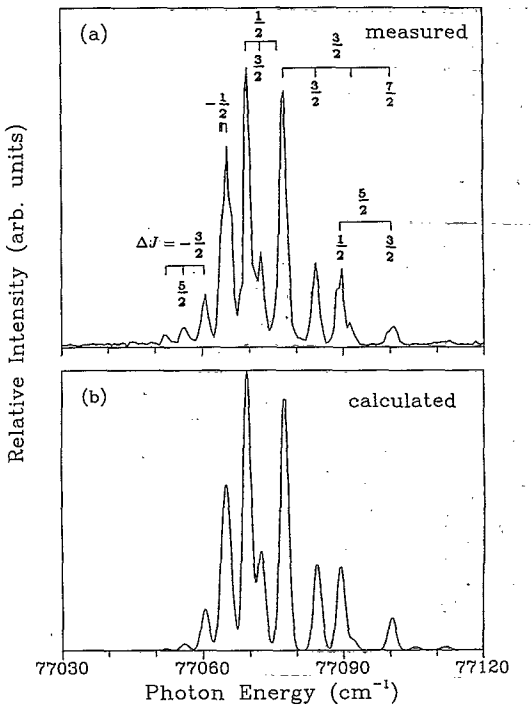

FIG. 2. (a) Measured and (b) calculated rotationally resolved threshold PFI photoelectron spectra for the single-photon ionization transition NO^+ $[X\,^1\Sigma^+(v^+=1,J^+)]+e^-\leftarrow NO$ $[X\,^2\Pi_{1/2}(v''=0,J'')]$. The rotational branch labels refer to $\Delta J=J^+-J''$. The calculated photoelectron spectrum assumes a ground state rotational temperature of 5 K.

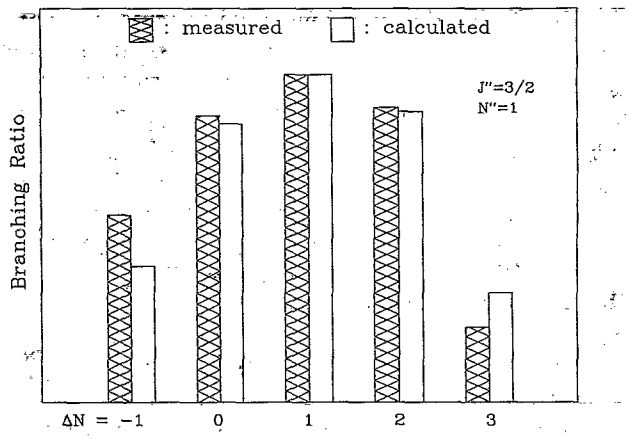

FIG. 3. (a) Measured and (b) calculated threshold ZEKE photoelectron spectra for single-photon ionization of the $N''=1$, $J''=3/2$ level of the $X\,^2\Pi_{1/2}$ state of NO by coherent VUV radiation (see text).

ground state rotational temperature of ~ 5 K as determined from comparison with *ab initio* calculations (discussed below). The narrowest observed linewidth is ~ 1.8 cm^{-1} (FWHM) which is primarily a result of the field-induced Stark shift. Using well known rotational constants for NO and NO^+ (Ref. 29), the PFI spectra are readily assigned to photoionization rotational branches on the basis of ΔJ, where $\Delta J=J^+-J''$. Hund's case (a) and case (b) are used to describe the angular momentum coupling for the neutral ground (J'') and ionic (J^+) states, respectively.[33] The energy scale of the displayed spectra is calibrated using the accurately determined ionization potential (IP) of NO (Refs. 34 and 35).

For the $v^+=1$ level [Fig. 2(a)], only small changes in total angular momentum are observed ($|\Delta J|\leqslant 5/2$) with branch intensities that fall off rapidly as $|\Delta J|$ increases. The corresponding $\Delta J=-5/2$ branch is missing in the $T_R=5$ K spectrum due to the small thermal population of rotational levels with $J''\geqslant 5/2$. This branch is observed in PFI spectra taken at higher T_R using 10%–15% NO in argon expansion mixtures. The intensity distribution in the $v^+=0$ spectrum (Fig. 1) is similar except for the intense line near 74 748 cm^{-1} and the weak PFI lines lying to the red end of the spectrum. The former corresponds to the $J^+=4\leftarrow J''=5/2$ transition while the latter fall at energies for $\Delta J=-3/2$ transitions leading to a band head near 74 700 cm^{-1}. The intensity of these $v^+=0$ levels is clearly not consistent with the low rotational temperature which characterizes the main part of the $v^+=0$ spectrum or the $v^+=1$ spectrum taken under identical expansion conditions. As in previous cases where intensity anomalies were suspected in ZEKE-PFI threshold photoelectron spectra,[14,15,36–38] it is likely that the rotational intensity distribution for the $v^+=0$ level is perturbed by autoionization of nearby low-n Rydberg states. The effects of autoionization in the $v^+=0$ spectrum is discussed in more detail at the end of this section.

The calculated near-threshold photoelectron spectra for rotationally cold $v^+=0$ and 1 levels are shown in Figs. 1(b) and 2(b), respectively. The best agreement with experiment was obtained with a ground state rotational temperature of $T_R=5$ K, which is consistent with experimental determinations of T_R from REMPI measurements on NO using similar expansion conditions and gas mixtures.[20,39] These spectra were calculated for a photoelectron energy of 50 meV and convoluted with a Gaussian detection function with a FWHM of 2 cm^{-1}. The calculated $v^+=1$ spectrum [Fig. 2(b)] agrees almost quantitatively with experiment, indicating that a one-electron description effectively describes the ionization dynamics. To provide further insight into the underlying dynamics of these ZEKE photoelectron spectra, Fig. 3 shows (a) measured and (b) calculated ion rotational branching ratios for photoionization of the $N''=1$, $J''=3/2$ rotational level of the $X\,^2\Pi_{1/2}$ ($v=0$) ground state of NO leading to the $X\,^1\Sigma^+$ ($v^+=1$) state of the ion. The experimental results shown here are estimated from the actual measured spectra of Fig. 2(a). These rotational branching ratios for ionization of a valence electronic state differ somewhat from those generally seen in ZEKE spectra of Rydberg states.

From conservation of angular momentum, the observation of branches with $|\Delta J|\leqslant 5/2$ implies that the photoelectron continuum at threshold is dominated by partial waves with $l\leqslant 1$ [$s(l=0)$ and $p(l=1)$]. This differs from expectations based on the calculated magnitudes $|D_l^{(-)}|$ of partial wave components of the photoelectron continuum shown in Fig. 4. Note that $|D_l^{(-)}|$ is the magnitude of only one of the μ components of $|r_{fi}^{\lambda\mu}|$ [see Eq. (4)]. Near

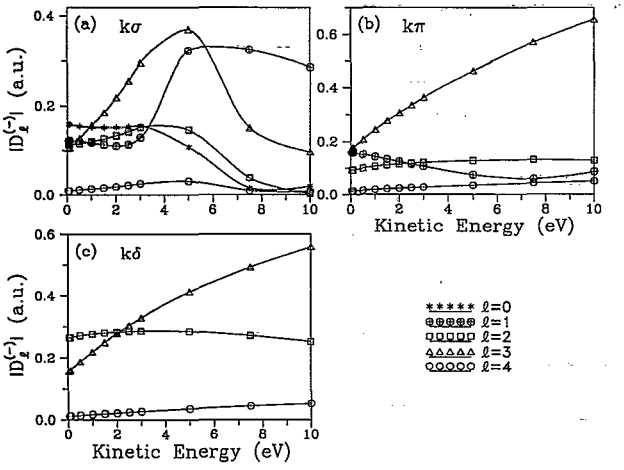

FIG. 4. Magnitude of the partial wave components of the photoelectron matrix element $|D_l^{(-)}|$ for photoionization of the $X\,^2\Pi$ ground state of NO. (a) $2\pi \rightarrow k\sigma$; (b) $2\pi \rightarrow k\pi$; and (c) $2\pi \rightarrow k\delta$ ionization channels.

threshold, these calculated $|D_l^{(-)}|$ show that $d(l=2)$ and $f(l=3)$ partial waves account for a substantial portion of the photoionization cross section. Given that these calculated photoelectron matrix elements yield an accurate representation of the measured threshold photoelectron spectra (see Figs. 2 and 3), one is led to the conclusion that photoexcitation into high l partial waves is not accompanied by *observable* changes in ion core angular momentum of comparable magnitude. That such large changes in angular momentum $\Delta J(N)$ are not seen in these spectra in spite of the significant magnitudes of the photoelectron matrix elements for higher $l(=3)$ is probably due to interference between these partial waves in the photoelectron continuum. The effect of such interference on ion rotational distributions has also been seen in spectra for $(2+1)$ REMPI via the $f\,^1\Pi(3p\sigma)$ and the $g\,^1\Delta(3p\pi)$ Rydberg states of NH.[40] However, this behavior is quite different from ion rotational distributions for threshold photoionization of O_2 which showed evidence for large changes in total angular momentum ($|\Delta J| \leqslant 9/2$) that could be attributed to a shape-resonance enhancement of the $f(l=3)$ partial wave of the $k\sigma$ continuum.[7,8] Note that the f partial wave shape resonance around 4–5 eV in the $k\sigma$ continuum [see Fig. 4(a)],[32] exerts little influence on the threshold photoionization.

It should also be noted that without resolving the Λ doublets (e/f) of the $X\,^2\Pi_{1/2}$ ground state rotational levels it is not possible to assign a specific parity (even or odd l) to individual rotational transitions as was done for REMPI measurements via several $^2\Sigma^+$ excited states of NO.[1–3,41,42] From Fig. 4, both even $(l=0,2)$ and odd $(l=1,3)$ partial waves are predicted to have significant photoionization oscillator strengths at threshold and both parities can contribute to each rotational transition. Since the 2π orbital of the $X\,^2\Pi$ ground state of NO has almost pure even [84.4% d and 9.9% g $(l_0=4)$] character, dominant odd partial wave contributions to the photoelectron matrix element are expected on the basis of an atomic-like propensity rule. The unusually strong even partial waves of the photoelectron (see Fig. 4) must arise from strong l mixing in the electronic continua caused by the nonspherical molecular ion potential.

The calculated $v^+=0$ threshold photoionization spectrum [Fig. 1(b)] is essentially identical to that for the $v^+=1$ state. This is expected since the photoionization transition moment does not have a significant dependence on internuclear distance. Furthermore, comparison of the experimental and calculated $v^+=0$ spectra highlights the perturbed intensity distribution of the observed $v^+=0$ rotational branches. As noted above, the enhanced intensity of certain transitions most likely arises from field-induced autoionization processes which are detected by the PFI measurement.[15,43] The mechanism involves the interaction of high-n Rydberg states $(\geqslant 150)$ with near degenerate low-n Rydberg states converging to higher cation rovibronic ionization limits. Application of the pulsed electric field lowers the ionization potential by an amount equal to the Stark shift and permits the mixed, low-n Rydberg states to autoionize. Field-induced autoionization has been used to explain anomalous rotational intensity profiles in previous PFI spectra of N_2O (Ref. 9), OH (Ref. 14), and HCl (Ref. 15).

The presence of the low-n Rydberg states which are responsible for such processes can often be observed in the absorption spectrum and/or the ion yield curve.[36,38] The NO^+ ion spectrum taken under similar expansion conditions and resolution is compared to the $v^+=0$ PFI spectrum in Fig. 5. Many of the features in the photoionization spectrum can be assigned to rotational transitions to the $8s,v=1$ and $4f,v=3$ Rydberg states observed in REMPI double-resonance measurements employing a very high resolution cw probe laser.[44] The appearance of the $8s,v=1$ level is unusual since it lies below the adiabatic ionization threshold and consequently cannot autoionize to $v^+=0$ rotational levels of the ion. Furthermore, the extraction field of 40 V/cm used to collect the ion spectrum in this work is too low to field ionize the $8s$ state. The observation of the $8s,v=1$ level in photoionization is attributed to the interaction with near degenerate high-n, $v=0$ Rydberg states which are field ionized by the extraction field.[44] It is likely that Rydberg state interactions are also responsible for the unexpected intensity of higher $J^+(=N^+)$ levels in the $\Delta J=-3/2$ and $-5/2$ branches of the PFI spectrum of NO. Many other unassigned autoionization features lie in the energy region of the strong rotational branch transitions involving low J^+ and it is reasonable to assume that the intensity distribution in the PFI spectrum is affected by their presence. As noted above, this is particularly evident for the $J^+=4 \leftarrow J''=5/2$ transition whose intensity is inconsistent with other members of the same rotational branch $(\Delta J=3/2)$ and the apparent low rotational temperature.

Finally, we note that the single-photon threshold photoelectron spectrum shown here for the unperturbed $v^+=1$ level (Fig. 2) is nearly identical to a recently published threshold spectrum for $v^+=0$ obtained by Strobel *et al.* via *two-photon* nonresonant ionization.[20] The similarity of one-

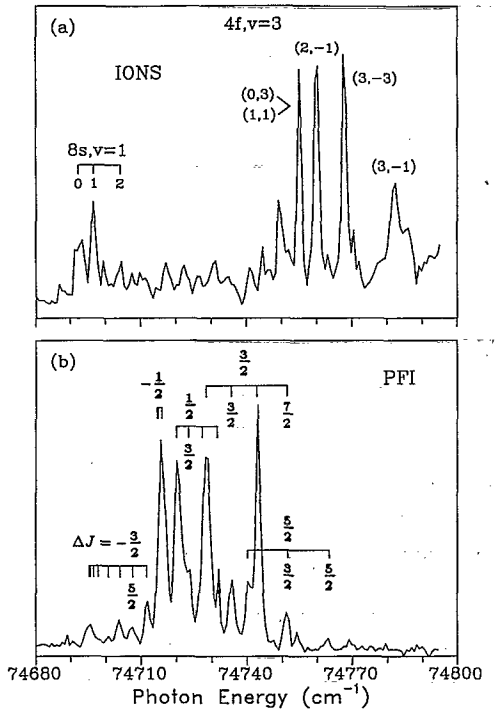

FIG. 5. Comparison of the VUV single-photon, PFI spectrum (b) and the total ion yield (a) near the adiabatic ionization threshold of NO. Both spectra were obtained under identical expansion conditions and the ground state rotational temperature is estimated to be ~5 K. Rotational levels of the $8s,v=1$ and $4f,v=3$ Rydberg states are shown. The notation for the $4f$ state corresponds to Hund's case (d) coupling, $(N^+,\mathcal{L})$, where N^+ is the ionic core rotational level and $\mathcal{L}$ is the projection of the orbital angular momentum of the $4f$ electron on the rotation axis (see Ref. 35).

and two-photon spectra is surprising since, at any given T_R, the two-photon spectrum is expected to exhibit additional rotational branches with larger ΔJ induced by the additional angular momentum of the second photon. A similar comparison has been made recently between the VUV one-photon[12] and two-photon, nonresonant threshold ionization of H_2S (Ref. 45). The two-photon spectrum for H_2S also has weak rotational branches with $\Delta N=\pm 2$, ± 3, whereas only $\Delta N=0, \pm 1$ transitions were observed in the one-photon spectrum. Differences in rotational branch intensities were also observed. The latter was attributed in part to accidental overlap with an intermediate excited state at the one-photon energy. For NO, the one-photon energy in the multiphoton ionization measurement (~37 360 cm^{-1}) lies well below the first electronically excited state [$A\,^2\Sigma^+(3s\sigma)$, T_{00}=44 200 cm^{-1}].[29] The two-photon spectrum for NO appears to be a more extreme case in which small angular momentum transfers are favored even though the partial wave distribution contains high l components.

ACKNOWLEDGMENTS

Work at Brookhaven National Laboratory was supported under Contract No. DE-AC02-76CH00016 with the U.S. Department of Energy and by its Division of Chemical Sciences, Office of Basic Energy Sciences. Work at the California Institute of Technology was supported by grants from the National Science Foundation, Air Force Office of Scientific Research, and the Office of Health and Environmental Research of the U.S. Department of Energy. We also acknowledge use of resources of the Jet Propulsion Laboratory/California Institute of Technology Y-MP2E/116 Supercomputer.

[1] W. G. Wilson, K. S. Viswanathan, E. Sekreta, and J. P. Reilly, J. Phys. Chem. **88**, 672 (1984); K. S. Viswanathan, E. Sekreta, E. R. Davidson, and J. P. Reilly, *ibid.* **90**, 5078 (1986); K. S. Viswanathan, E. Sekreta, and J. P. Reilly, *ibid.* **90**, 5658 (1986).
[2] X. Song, E. Sekreta, J. P. Reilly, H. Rudolph, and V. McKoy, J. Chem. Phys. **91**, 6062 (1989); H. Rudolph and V. McKoy, *ibid.* **91**, 2235 (1989).
[3] K. Wang, J. A. Stephens, and V. McKoy, J. Chem. Phys. **95**, 6456 (1991).
[4] K. L. Reid, D. J. Leahy, and R. N. Zare, Phys. Rev. Lett. **68**, 3527 (1992).
[5] K. Müller-Dethlefs and E. W. Schlag, Annu. Rev. Phys. Chem. **42**, 109 (1991).
[6] G. Reiser, W. Habenicht, K. Müller-Dethlefs, and E. W. Schlag, Chem. Phys. Lett. **152**, 119 (1988).
[7] R. G. Tonkyn, J. W. Winniczek, and M. G. White, Chem. Phys. Lett. **164**, 137 (1989).
[8] M. Braunstein, V. McKoy, S. N. Dixit, R. G. Tonkyn, and M. G. White, J. Chem. Phys. **93**, 5345 (1990).
[9] R. T. Wiedmann, E. R. Grant, R. G. Tonkyn, and M. G. White, J. Chem. Phys. **95**, 746 (1991).
[10] R. G. Tonkyn, R. T. Wiedmann, E. R. Grant, and M. G. White, J. Chem. Phys. **95**, 7033 (1991).
[11] M.-T. Lee, K. Wang, V. McKoy, R. G. Tonkyn, R. T. Wiedmann, E. R. Grant, and M. G. White, J. Chem. Phys. **96**, 7848 (1992).
[12] R. T. Wiedmann and M. G. White, in *Proceedings of the SPIE: Optical Methods for Time- and State-Resolved Chemistry* (SPIE, Bellingham, WA, 1992), Vol. 1638, p. 273.
[13] K. Wang, M.-T. Lee, V. McKoy, R. T. Wiedmann, and M. G. White (in preparation).
[14] R. T. Wiedmann, R. G. Tonkyn, M. G. White, K. Wang, and V. McKoy, J. Chem. Phys. **97**, 768 (1992).
[15] R. G. Tonkyn, R. T. Wiedmann, and M. G. White, J. Chem. Phys. **96**, 3696 (1992).
[16] A. D. Buckingham, B. J. Orr, and J. M. Sichel, Philos. Trans. R. Soc. London, Ser. A **268**, 147 (1970).
[17] J. Xie and R. N. Zare, J. Chem. Phys. **93**, 3033 (1990).
[18] M. Braunstein, S. N. Dixit, and V. McKoy, J. Chem. Phys. **96**, 5726 (1992).
[19] M.-T. Lee, K. Wang, and V. McKoy, J. Chem. Phys. **97**, 3108 (1992).
[20] A. Strobel, I. Fischer, J. Staeker, G. Nieder-Schatteburg, K. Müller-Dethlefs, and V. Bondybey, J. Chem. Phys. **97**, 2332 (1992).
[21] R. G. Tonkyn and M. G. White, Rev. Sci. Instrum. **60**, 1245 (1989).
[22] C. E. Moore, *Atomic Energy Levels* (U.S. GPO, Washington, D.C., 1971), Vol. II, p. 170.
[23] R. Hilbig, G. Hilber, A. Lago, B. Wolff, and R. Wallenstein, in *Short Wavelength Coherent Radiation: Generation and Applications*, edited by R. G. Lerner (American Institute of Physics, New York, 1986), p. 382.
[24] J. Berkowitz, *Photoabsorption, Photoionization and Photoelectron Spectroscopy* (Academic, New York, 1979), p. 89.
[25] W. A. Chupka (private communication).
[26] K. Wang and V. McKoy, J. Chem. Phys. **95**, 4977 (1991).
[27] S. N. Dixit and V. McKoy, J. Chem. Phys. **82**, 3546 (1985).
[28] A. R. Edmonds, *Angular Momentum in Quantum Mechanics* (Princeton University, Princeton, 1974).
[29] K. P. Huber and G. Herzberg, *Molecular Spectra and Molecular Structure, IV. Constants of Diatomic Molecules* (Van Nostrand, New York, 1979).
[30] T. H. Dunning, Jr., J. Chem. Phys. **53**, 2823 (1970).
[31] R. R. Lucchese, G. Raseev, and V. McKoy, Phys. Rev. A **25**, 2572 (1982).
[32] M. E. Smith, R. R. Lucchese, and V. McKoy, J. Chem. Phys. **79**, 1360 (1983).

[33] G. Herzberg, *Molecular Spectra and Molecular Structure, I. Spectra of Diatomic Molecules* (Van Nostrand, New York, 1950), Chap. V.
[34] E. Miescher, Can. J. Phys. **54**, 2074 (1976).
[35] D. Th. Biernacki, S. D. Colson, and E. E. Eyler, J. Chem. Phys. **88**, 2099 (1988).
[36] F. Merkt and T. P. Softley, J. Chem. Phys. **96**, 4149 (1992).
[37] G. Reiser and K. Müller-Dethlefs, J. Phys. Chem. **96**, 9 (1992).
[38] G. P. Bryant, Y. Jiang, M. Martin, and E. R. Grant, J. Phys. Chem. **97**, 6875 (1992).
[39] J. R. Appling, M. G. White, W. J. Kessler, R. Fernandez, and E. D. Poliakoff, J. Chem. Phys. **88**, 2300 (1988).
[40] K. Wang, J. A. Stephens, V. McKoy, E. de Beer, C. A. de Lange, and N. P. C. Westwood, J. Chem. Phys. **97**, 211 (1992).
[41] S. W. Allendorf, D. J. Leahy, D. C. Jacobs, and R. N. Zare, J. Chem. Phys. **91**, 2216 (1989).
[42] M. Sander, L. A. Chewter, K. Müller-Dethlefs, and E. W. Schlag, Phys. Rev. A **36**, 4543 (1987).
[43] R. D. Gilbert and M. S. Child, Chem. Phys. Lett. **187**, 153 (1991).
[44] D. Th. Biernacki, Ph.D. thesis, Yale University, 1988.
[45] I. Fischer, A. Lochschmidt, A. Strobel, G. Niedner-Shatteburg, K. Müller-Dethlefs, and V. E. Bondybey, J. Chem. Phys. (submitted).